Prediction of tower loading of floating offshore wind turbine systems in the extreme wind and wave conditions

Nan Xu*[1] and Takeshi Ishihara[2]

[1]Research Fellow, Engineering Consulting Department, China Academy of Building Research, 30# Bei San Huan Dong Lu, Beijing, 100013 China, Fax:+86-84279246, E-mail:nanxu08@sina.com

[2]Professor, Department of Civil Engineering, The University of Tokyo

Received 11/26/2013; Revised 06/17/2014; Accepted 06/20/2014

ABSTRACT

The analytical formulae of wind-induced load, wave-induced load and their combination are proposed for the tower of floating offshore wind turbine systems by quasi-steady analysis. Sway-rocking model (SR model) is employed as the equivalent calculation model. The formulae of wind-induced load are in the same format as those of fixed-foundation wind turbine, but have different values for some critical parameters in resonant standard deviation. For wave-induced load, the standard deviations due to surge and pitch motions are proposed separately and their combination is calculated with complete quadratic combination (CQC) rule. For the total tower loading under wind and wave, the mean value depends on the wind only, and the combination without considering any correlation can predict the standard deviation accurately. The Gaussian peak factor is applicable to both wave-induced load and the total tower loading. All the proposed formulae are verified by full dynamic simulation.

Keywords: Quasi-steady analysis, Analytical formulae, Sway-rocking model (SR model), Wind-induced load, Wave-induced load, Loads combination, Floating offshore wind turbine

1. INTRODUCTION

The offshore consists of a vast wind resource in deep water, where use of conventional bottom-mounted wind turbines is not possible, and floating wind turbines are the most attractive [1–2]. The extreme wind and wave conditions are more dominant than the normal conditions for the maximum loading on the support structure of wind turbine in Japan. It is found by full dynamic simulation that floater motion increases the tower loading compared to land-based wind turbine under the same wind conditions. Thus, it is necessary to consider the wave effect on the tower loading to check the serviceability of the wind turbines which are designed for the bottom-mounted systems. Since in the extreme conditions the aerodynamic force due to the wave-induced motion can be neglected, which means the coupling of wind-induced load and wave-induced load is very weak, in the preliminary design it would make sense for each kind of load to be investigated independently, and then their combination can be performed to get the final design value. In order to propose the analytical formulae for the loads estimation by quasi-steady analysis, a reasonable calculation model of floating offshore wind turbine system is necessary.

In this study, loads evaluation methods are discussed in Section 2; In Section 3, a sway-rocking model (SR model) [3] is employed as the equivalent calculation model of a floating offshore wind turbine system. The complex mooring system is modeled as two kinds of springs and dampers. The stiffness and damping should be determined by free vibration simulation. In Section 4, the analytical formulae for the estimation of wind-induced load and wave-induced load are proposed with the SR

model by quasi-steady analysis. Section 5 presents the combination of wave-induced load and wind-induced load. It is shown that the combination without considering any correlation can predict the tower loading accurately. All the proposed formulae are verified by full dynamic simulation.

2. LOADS EVALUATION METHODS

In the previous study, the wind-induced tower loading can be evaluated by either full dynamic simulation or quasi-steady analysis [4], and wave-induced tower loading is usually evaluated by full dynamic simulation [5]. This study will investigate the quasi-steady analysis for both kinds of loads and propose the analytical formulae to make the application more convenient and identify the dominant influence factors as well. Hence, this study would be very useful for the optimization of floating wind turbine systems. The full dynamic simulation is used as the validation of the proposed formulae.

2.1. Quasi-steady analysis

A coefficient called peak factor proposed by Davenport [6] to account for fluctuating wind load is used in quasi-steady analysis for wind and wave induced loads in this study. The maximum bending moment is estimated by eqn (1).

$$M = \overline{M} + \sigma \cdot g \tag{1}$$

where $\overline{M}$ is the mean bending moment, σ is the standard deviation, g is the peak factor.

The assumptions used in this study are listed below:

1. For wave-induced load, the floater and wind turbine (three blades, hub, nacelle, tower) can be modeled as 11 lumped masses in order to give a clear explanation about the tower loading, since the aerodynamic force is not considered. The three blades are regarded as rigid approximately and can be modeled as a concentrated mass above the tower top with hub and nacelle together. The tower is divided into 10 masses with the floater mass added to the tower base.
2. Only the first mode is considered in the respective calculation of tower loading due to surge and pitch motions because the first mode is much more dominant.
3. The peak factor is proposed considering the response of the whole wind turbine, so it doesn't change with height. The bending moment-based peak factor in this study can be used for the calculation of shear force on the wind turbine tower.

2.2. Full dynamic simulation

A fully nonlinear dynamic simulation code CAsT [5] is used to investigate the dynamic response of floating offshore wind turbine systems considering the coupled interaction between wind turbine, floater and mooring system. A summary of this numerical scheme is presented in Table 1. CAsT has been verified by a water tank experiment, thus can give accurate and realistic prediction of floater motion and tower loading due to wind and wave. This study employs CAsT to simulate the floater motion and verify the analytical solution of tower loading. The general formulation of the differential equation of motion for the structure is given at eqn (2):

$$[M]\ddot{x} + [C]\dot{x} + [K]x = [F] \tag{2}$$

where $[M]$ is the mass matrix, $[C]$ is the damping matrix, $[K]$ is the stiffness matrix, $[F]$ is the external force matrix.

2.3. Wind turbine system

This study uses a semi-submersible type floater installed with 5-MW baseline wind turbine developed by NREL (National Renewable Energy Laboratory) and catenary mooring system to investigate the tower loading in the extreme wind and wave conditions. The details of the floater are given by Waris [5], and Jonkman [7] presents the details of the wind turbine. The salient features of floater and basic properties of wind turbine are summarized in Table 2.

The catenary mooring system is considered to consist of three mooring lines, each having span of 400 m. The mooring lines are separated at 120°, with front two lines having an angle of 60° with the incident wind and wave, and the third aligned in the wind and wave direction. All the three lines have a common fairlead at the base of the central column of the floater that supports the wind turbine on top. The catenary mooring arrangement is shown in Figure 1.

Table 1. Description of the full dynamic simulation code CAsT [5]

Name	Description
Eigenvalue analysis	Subspace iteration procedure
Dynamic Analysis	Direct Implicit Integration (Newmark-β)
Formulation	Total Lagrangian formulation
Convergence	Newton-Raphson Method
Damping Estimation	Rayleigh damping model
Element Type	Beam (12-DOF), Truss (8-DOF)
Aerodynamic force	Quasi-steady aerodynamic theory
Hydrodynamic Force	Morison Equation + Srinivasan Model
Restoring Force	Non-Hydrostatic Model
Mooring Force	Nonlinear
Seabed contact	Penalty Method

Table 2. Floating wind turbine description [5, 7]

Name	Detail	Description
Semi-submersible floater	Span (m)	60.0
	Submerged Depth (m)	20.0
	Overall Height (m)	30.0
5MW wind turbine	Rotor radius R (m)	63.0
	Hub height H_h (m)	90.0
	1st frequency n_t (Hz)	0.262
	Rotor (including nacelle) mass m_r (kg)	350000
	Tower mass m_t (kg)	347460
Wind turbine+floater	1st modal mass m_1 (kg)	4524796

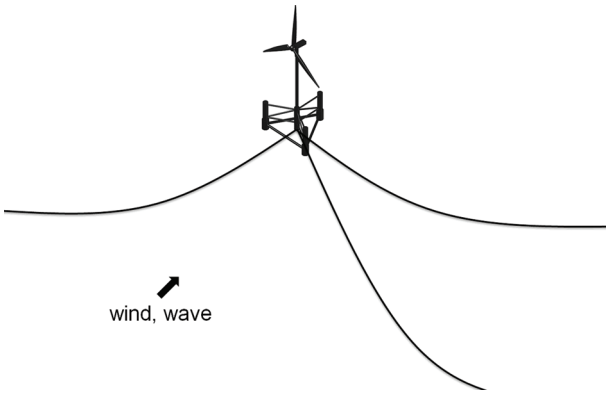

Figure 1. Catenary mooring system analyzed in this study

3. SWAY-ROCKING MODEL

Since surge and pitch are two dominant floater motions under wind and wave [5], the SR model is used as the equivalent calculation model to predict the tower loading. As shown in Figure 2(a), the complex mooring system of floating wind turbine system is modeled as two kinds of springs and dampers. Surge motion (sway) can be represented with the lateral spring and pitch motion (rocking) with rotational spring. Different from the SR model in earthquake engineering, stiffness k_S, k_R and damping c_S, c_R should be determined by free vibration simulation in this study. An extra vertical force is added to consider the weight of the mooring system, offsetting the difference of buoyancy and the weight of wind turbine and floater. It is noted that the full wind turbine model of Figure 2(a) has to be used for the estimation of wind-induced load, while the lumped masses of Figure 2(b) can be used to determine the stiffness and damping, and also for the estimation of wave-induced load. The lumped masses are listed in Table 3.

Taking the superstructure (wind turbine and floater) as rigid body, the sway frequency ω_S and rocking frequency ω_R can be obtained by free vibration simulation using full dynamic simulation. Thus, the stiffness of the two springs can be calculated as follows [8]:

$$k_S = \left(\sum_{i=1}^{n} m_i \right) \omega_S{}^2, \qquad k_R = \left(\sum_{i=1}^{n} m_i h_i^2 \right) \omega_R{}^2 \tag{3a, 3b}$$

where h_i is the height from the tower base.

From the displacement time series of free vibration simulation, the sway damping ratio ξ_S and rocking damping ratio ξ_R can be recognized as well. Thus, the damping of the two dampers can be calculated as follows:

$$c_S = 2\left(\sum_{i=1}^{n} m_i \right) \omega_S \xi_S, \qquad c_R = 2\left(\sum_{i=1}^{n} m_i h_i^2 \right) \omega_R \xi_R \tag{4a, 4b}$$

The comparison of the first natural periods between SR model and full model with catenary are tabulated in Table 4. The comparison of the first mode shape along tower is shown in Figure 3, and 1 is assumed for rotor. It is noticed that SR model is able to give very close natural periods and mode shape to the full model.

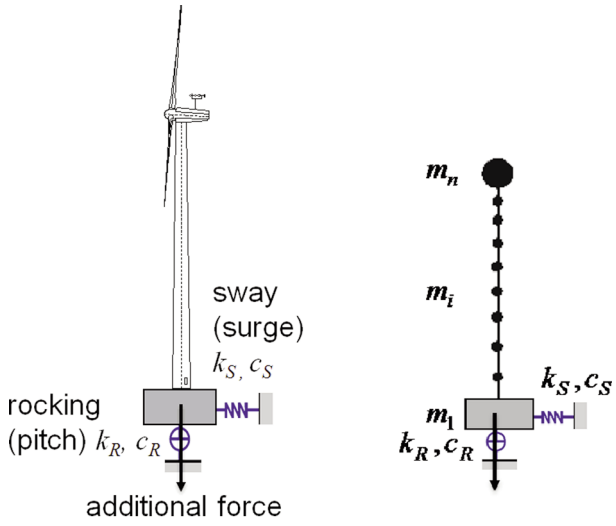

Figure 2. Sway-rocking model

Table 3. Lumped mass of wind turbine

Height from tower base h_i (m)	Lumped mass m_i (kg)
0	4134403.52
8.76	45861.86
17.52	42825.06
26.28	39891.40
35.04	37060.89
43.80	34333.51
52.56	31709.23
61.32	29188.10
70.08	26770.12
78.84	24455.25
87.60	361661.80

Table 4. Comparison of the first natural periods

Motion	Full model/SR model
Surge	26.8s/26.2s
Pitch	14.3s/15.0s

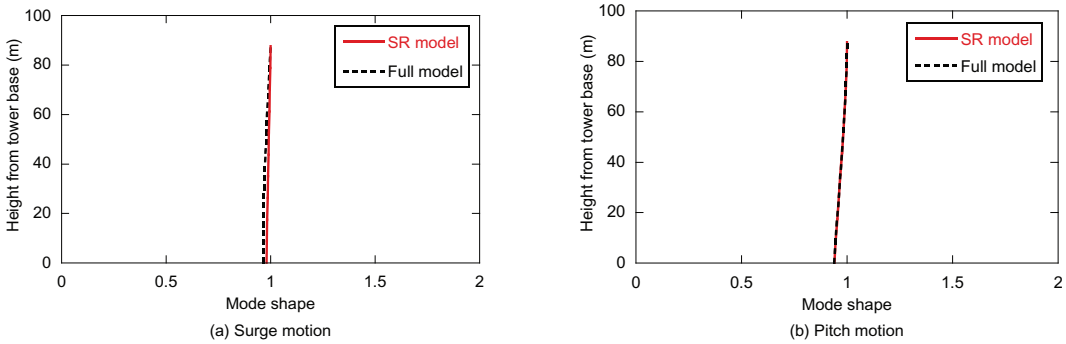

Figure 3. Comparison of the first mode shape with full model

4. EVALUATION OF WIND-INDUCED LOAD AND WAVE-INDUCED LOAD

The wind-induced load and wave-induced load can be investigated independently in the preliminary design due to their weak coupling in the extreme condition, and then their combination can be performed to get the final design value. In this section, the analytical formulae of these two kinds of loads are proposed respectively based on SR model and quasi-steady analysis.

4.1. Wind-induced load

The analytical formulae of wind-induced load derived based on the SR model and quasi-steady analysis have been proposed by Xu [4], which are in the same format as those of fixed-foundation wind turbine [9]. This paper just gives a brief summary of the comparison between fixed-foundation wind turbine and floating wind turbine, and refers to Xu [4, 9] for details. From analytical formulae, it is easily found that the mean wind load and background standard deviation are the same since they only depend on the wind itself; however, the resonant standard deviation is different since it is determined by structural vibration characteristics. It is noticed that the first natural frequency and damping ratio of the system are dominant influence factors, and floating wind turbine has much different values from the fixed-foundation wind turbine in these two factors. The non-Gaussian peak factor is found to be not sensitive to the type of foundation. The SR model is considered as the consistent calculation model of wind load, which can consider any type of wind turbine foundation by changing the stiffness and damping, and it becomes the fixed-foundation model when the stiffness is infinite.

4.2. Wave-induced load

In the real situation, the irregular wave which is represented by the significant wave height H_s and the spectral peak period T_p should be used. In this study the extreme 3-hour sea state with a 50-year recurrence period is considered. In the short term, i.e. over a 3-hour or 6-hour period, stationary wave conditions with constant H_s and constant T_p are assumed to prevail [10]. Thus, significant wave height 10.75 m and peak wave period varying from 10~20 sec at an interval of 1s are used in this paper. The time history of wave elevation is generated using model developed by Chaplin [11] for JONSWAP spectrum. The peak factor of wave is determined as 3.3; the shape factor is 0.07 for $\omega \le 2\pi/T_p$ and 0.09 for $\omega > 2\pi/T_p$ according to Chakrabarti [12]. Here, ω is the angular frequency of wave.

The full dynamic simulation indicates that the wave-induced mean load on the tower is close to 0 [5], therefore, the wave-induced maximum load becomes the product of standard deviation and peak factor in eqn (1). Modal analysis is used to determine the standard deviation, in which the effects of floater surge and pitch motions are investigated separately by locking the other motion in the SR model, and then their combination is performed to get the total standard deviation.

A Gaussian peak factor is proposed since the tower loading due to the wave-induced background motion which is Gaussian process is much more dominant compared to those due to the peak acceleration of floater motions and resonance of tower.

4.2.1. Standard deviation

By locking the pitch motion as shown in Figure 4 (a), the modal equation of motion of *j* th mode in surge direction is [8]:

$$M_j^S \ddot{f}_j^S(t) + C_j^S \dot{f}_j^S(t) + M_j^S \omega_j^{S2} f_j^S(t) = \begin{bmatrix} \phi_{nj}^S \\ \vdots \\ \phi_{1j}^S \end{bmatrix}^T \begin{bmatrix} 0 \\ \vdots \\ F_{wave}(t) \end{bmatrix} = \phi_{1j}^S F_{wave}(t) \quad (j = 1, \cdots, n) \tag{5}$$

where $M_j^S = \sum_{k=1}^{n} m_k \phi_{kj}^{S2}$ is the generalized mass, $C_j^S = \sum_{k=1}^{n} c_k \phi_{kj}^{S2}$ $(c_1 = c_S)$ is the generalized damping and ω_j^s is the modal natural frequency in radians per second, f_j^s is the modal displacement, ϕ_j^s $(k = 1, \ldots, n)$ is the normalized mode shape of the *jth* mode, and F_{wave} (t) is the equivalent wave force in surge direction.

If the wave varies harmonically, the modal displacement $f_j^S(t)$ can be shown as [8]:

$$f_j^S(t) = \phi_{1j}^S F_{wave}(t) \left| H_j^S(\omega) \right| \tag{6}$$

where $\left| H_j^S(\omega) \right| = \dfrac{1}{M_j^S \omega_j^{S2} \sqrt{\left(1 - \beta_j^{S2}\right)^2 + 4\xi_j^{S2} \beta_j^{S2}}}$, $\beta_j^S = \dfrac{\omega}{\omega_j^S}$, $\xi_j^S = \dfrac{C_j^S}{2M_j^S \omega_j^S}$.

β_j^S is the ratio between external wave frequency ω and structural natural frequency, and ξ_j^S is the damping ratio, which is taken as the summation of structural damping ratio and hydrodynamic damping ratio.

In modal analysis the excitations of the various different natural modes of vibration are computed separately and the results superposed. In surge direction, substituting (6) the acceleration at node *k* can be calculated as:

$$\ddot{x}_k^S = \sum_{j=1}^{n} \ddot{f}_j^S(t) \phi_{kj}^S = -\omega^2 F_{wave}(t) \sum_{j=1}^{n} \left| H_j^S(\omega) \right| \phi_{1j}^S \phi_{kj}^S \tag{7}$$

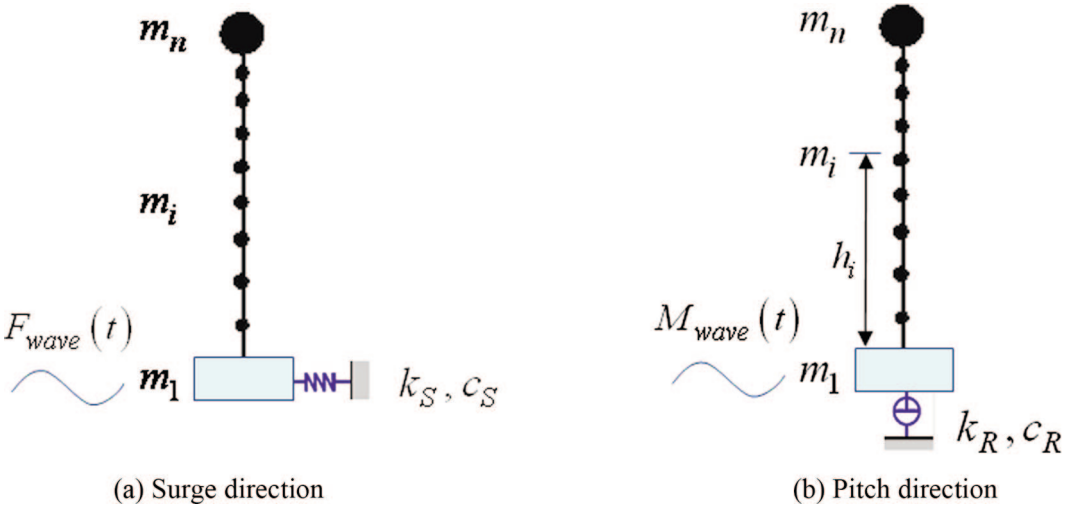

(a) Surge direction (b) Pitch direction

Figure 4. Calculation model used in the modal analysis

If only the first mode is considered, the shear force at node i is derived as:

$$Q_i^S(t) = \sum_{k=i}^{n} m_k \ddot{x}_k^S \approx \sum_{k=i}^{n} m_k a_S(t) \left(1 + \frac{\Delta\phi_{k1}^S}{\phi_{11}^S}\right) \tag{8}$$

where $a_S(t)$ is the known surge acceleration at tower base, which can be provided by the ocean engineer in the real project, and in this study it is obtained from full dynamic simulation. $\Delta\phi_{k1}^S = \phi_{k1}^S - \phi_{11}^S$ and $\Delta\phi_{k1}^S/\phi_{11}^S$ is defined as the elastic/solid ratio of mode shape at node k.

From eqn (8) it is found that the shear force consists of a solid part and an elastic part. The elastic part is the function of $\Delta\phi_{k1}^S/\phi_{11}^S$. The mode shape changes with the stiffness k_S of surge spring, as shown in Figure 5. Take the elastic/solid ratio of mode shape at tower top $\Delta\phi_{n1}^S/\phi_{11}^S$ as indicator. $\Delta\phi_{n1}^S/\phi_{11}^S$ increases when the stiffness k_S increases, which means that the shear force increases when the stiffness k_S increases if the surge acceleration $a_S(t)$ keeps constant.

From eqn (8) the standard deviations of shear force and bending moment σ_i^{QS} and σ_i^{MS} due to surge motion can be calculated from the standard deviation of surge acceleration σ_{aS}:

$$\sigma_i^{QS} = \sum_{k=i}^{n} m_k \sigma_{aS} \left(1 + \frac{\Delta\phi_{k1}^S}{\phi_{11}^S}\right) \tag{9}$$

$$\sigma_i^{MS} = \sum_{k=i}^{n} m_k (h_k - h_i) \sigma_{aS} \left(1 + \frac{\Delta\phi_{k1}^S}{\phi_{11}^S}\right) \tag{10}$$

For pitch direction shown in Figure 4 (b), the linear acceleration at node k can be calculated as:

$$\ddot{x}_k^P = \sum_{r=1}^{k-1} \ddot{\theta}_r^P (h_{r+1} - h_r) \tag{11}$$

where $\ddot{\theta}_r^P$ is the angular acceleration at node r, which can be obtained from modal analysis as well, referring to the *Appendix* for the details of the derivation. Like surge direction, if only the first mode is considered the shear force at node i can also be obtained from the known pitch acceleration at tower base $a_P(t)$:

$$Q_i^P(t) = \sum_{k=i}^{n} m_k \ddot{x}_k^P = \sum_{k=i}^{n} m_k a_P(t) \left(h_k + \sum_{r=1}^{k-1} \frac{\Delta\phi_{r1}^P}{\phi_{11}^P}(h_{r+1} - h_r)\right) \tag{12}$$

where $\Delta\phi_{r1}^P = \phi_{r1}^P - \phi_{11}^P$. $\Delta\phi_{r1}^P/\phi_{11}^P$ is defined as the elastic/solid ratio of mode shape at node r.

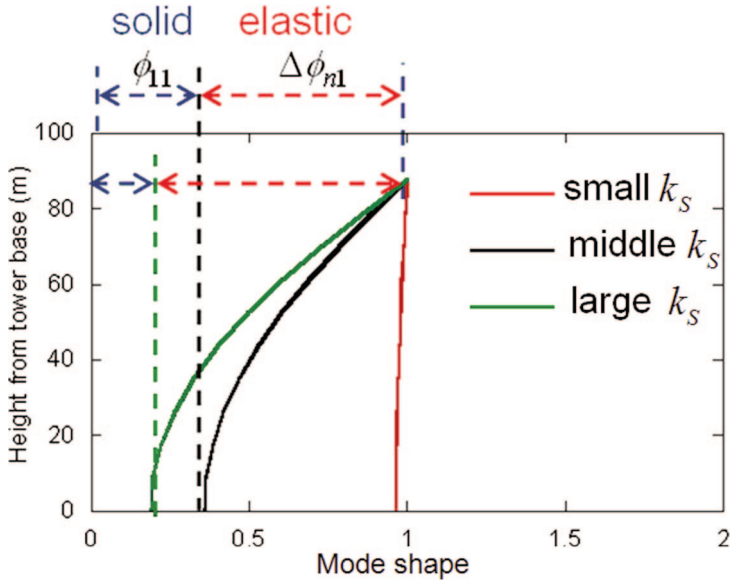

Figure 5. Variation of mode shape with stiffness k_S

Then the standard deviations of shear force and bending moment σ_i^{QP} and σ_i^{MP} due to pitch motion can be calculated from the standard deviation of pitch acceleration σ_{aP}:

$$\sigma_i^{QP} = \sum_{k=i}^{n} m_k \sigma_{aP} \left(h_k + \sum_{r=1}^{k-1} \frac{\Delta\phi_{r1}^P}{\phi_{11}^P} \left(h_{r+1} - h_r \right) \right) \tag{13}$$

$$\sigma_i^{MP} = \sum_{k=i}^{n} m_k g \sigma_{\theta P} \left(h_k + \sum_{r=1}^{k-1} \frac{\Delta\phi_{r1}^P}{\phi_{11}^P} \left(h_{r+1} - h_r \right) \right) + \sum_{k=i}^{n} m_k \left(h_k - h_i \right) \sigma_{aP} \left(h_k + \sum_{r=1}^{k-1} \frac{\Delta\phi_{r1}^P}{\phi_{11}^P} \left(h_{r+1} - h_r \right) \right) \tag{14}$$

The first term in the right hand side of eqn (14) considers the P–Δ effect caused by the pitch angle, where $\sigma_{\theta P}$ is the standard deviation of pitch angle of tower base in radian.

Both surge and pitch motions have significant effect on the tower loading of catenary system. Hence, the influence of the two motions should be combined together. From the full dynamic simulation, it is recognized that the maximum responses of surge and pitch don't occur concurrently, but a certain correlation exists between them. Referring to the seismic loads specified in AIJ [13], complete quadratic combination (CQC) is used here for the combination, as surge and pitch modes have closer eigenvalues. Therefore, the total standard deviations of shear force and bending moment are calculated as:

$$\sigma_i^Q = \sqrt{\left(\sigma_i^{QS}\right)^2 + \rho_{SP} \sigma_i^{QS} \sigma_i^{QP} + \left(\sigma_i^{QP}\right)^2} \tag{15}$$

$$\sigma_i^M = \sqrt{\left(\sigma_i^{MS}\right)^2 + \rho_{SP} \sigma_i^{MS} \sigma_i^{MP} + \left(\sigma_i^{MP}\right)^2} \tag{16}$$

where ρ_{SP} is the correlation factor between surge and pitch modes.

$$\rho_{SP} = \frac{8\sqrt{\xi_S \xi_P}\left(\xi_S + r_{SP}\xi_P\right) r_{SP}^{3/2}}{\left(1 - r_{SP}\right)^2 + 4\xi_S \xi_P r_{SP}\left(1 + r_{SP}^2\right) + 4\left(\xi_S^2 + \xi_P^2\right) r_{SP}^2} \tag{17}$$

where ξ_S, ξ_P are the damping ratios of surge and pitch, respectively. $r_{SP} = \omega_S/\omega_P$ is the ratio between the natural frequency of surge and pitch modes. Therefore, the correlation between surge and pitch modes doesn't change with the external excitation, i.e., wave force, and it only depends on the damping and natural frequency of the system. Here, $\xi_S = 0.20$, $\xi_P = 0.21$, $\omega_S = 0.26$, $\omega_P = 0.37$ have been obtained from the free vibration simulation. Thus, $\rho_{SP} = 0.79$ is calculated.

Figure 6 shows that the proposed formulae agree well with the full dynamic simulation for the standard deviation of wave-induced load on tower. It is found that the standard deviations of shear force and bending moment decrease with the peak period of wave.

4.2.2. Peak factor

It is noted here that the peak factor is proposed considering the response of the whole wind turbine, so it doesn't change with height. The bending moment-based peak factor in this study can be used for the calculation of shear force on the wind turbine tower. Figure 7 shows the comparison of power spectrum density of tower base bending moment for the wave peak periods: 10 s, 15 s and 20 s. It is noted that the dynamic tower loading consists of three parts. Taking the 10 s case as

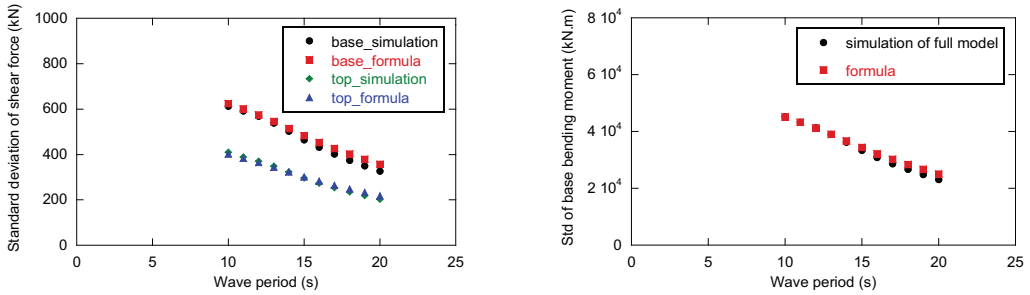

(a) Standard deviation of shear force on tower base and top

(b) Standard deviation of bending moment on tower base

Figure 6. Comparison of standard deviation of wave-induced load with full dynamic simulation

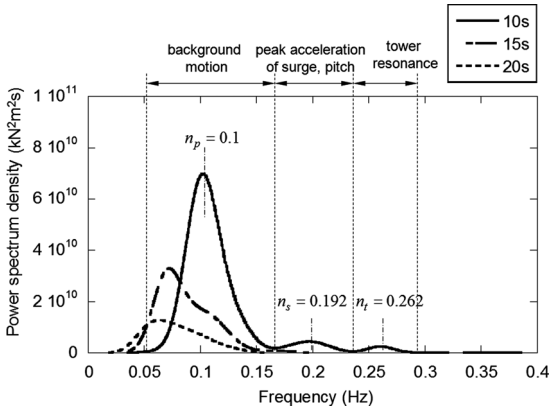

Figure 7. Comparison of power spectrum density of tower base bending moment

example, the range around the first peak is caused by wave-induced background motion of floater, which has the same peak frequency as wave $n_p = 0.1$; The range around the second peak is due to the peak acceleration of the floater surge and pitch motions with the peak frequency $n_s = 0.192$; The range around the third peak is the resonant part due to the tower vibration with the peak frequency $n_t = 0.262$, corresponding to the first natural period of tower 3.8s. The second and third peaks are negligibly small compared to the first peak, since they are only slightly excited by wave. In 15s case and 20s case, the second and third peaks will not exist, leaving the first peak only, since the frequency difference from the wave becomes larger and external excitation becomes weaker. That is the reason why the skewness α_3 of tower base bending moment obtained from the full dynamic simulation (Figure 8) is close to zero, which follows the skewness of wave. As a result a Gaussian process can be assumed for the tower base bending moment of floating wind turbine, and the Gaussian peak factor of eqn (18) can be used.

$$g = \sqrt{2\ln(\nu_0 T)} + \frac{0.5772}{\sqrt{2\ln(\nu_0 T)}} \tag{18}$$

where ν_0 is the zero up-crossing frequency of tower base bending moment for Gaussian process:

$$\nu_0 = \sqrt{\frac{\int_0^\infty n^2 S(n)\,dn}{\int_0^\infty S(n)\,dn}} \approx \sqrt{\frac{n_p^2\sigma_b^2 + n_s^2\sigma_s^2 + n_t^2\sigma_t^2}{\sigma_b^2 + \sigma_s^2 + \sigma_t^2}} \tag{19}$$

where n is the frequency in Hertz, and $S(n)$ is the power spectrum density. Since the three parts of the spectrum in Figure 7 are all narrow band, the integration in eqn (19) can also be written into three parts approximately. σ_b^2, σ_s^2 and σ_t^2 are the variance of background motion part, peak acceleration part and tower resonant part, respectively. As discussed before, σ_s^2 and σ_t^2 are negligibly small compared to σ_b^2. Hence, the zero up-crossing frequency becomes $\nu_0 = n_p$ approximately. It is indicated in Figure 9 that the Gaussian peak factor agrees well with full dynamic simulation and it doesn't change much with wave period.

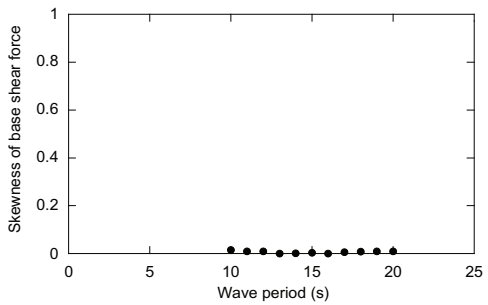

Figure 8. Skewness of tower base bending moment

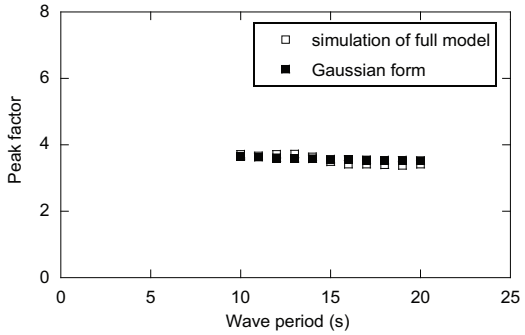

Figure 9. Comparison of peak factors between simulation and formula

5. COMBINATION OF WIND-INDUCED LOAD AND WAVE-INDUCED LOAD

This section presents the combination of wind-induced load and wave-induced load. The reason why the assumption of perfect correlation between them causes overestimation has been clarified. It is shown that the combination without considering any correlation can predict the tower loading accurately.

5.1. Correlated wind and wave conditions

For DLC 6.1a, the turbulent extreme wind model shall be taken together with the extreme sea state conditions [10]. The full dynamic simulation carries on six 1-hour realizations for each combination of extreme wind speed and extreme sea state. In this case, the hub height mean wind speed, turbulence standard deviation and significant wave height shall be taken as 50-year recurrence values each referenced to a 1-hour simulation period. The hub height mean wind speed of 10 min value is considered as 40~50 m/s. Further, for representation of turbulent wind speeds, the turbulent extreme wind model makes use of characteristic turbulence intensity 0.11, which is 10 min value at hub height [14, 15].

In this study, the SMB method [16–18] is used to consider the correlation between the mean wind speed U_{10} at 10 m height from the sea level and the significant wave height H_s and wave peak period T_P:

$$H_s = \alpha H_{0,SMB} + (1-\alpha) H_{0,swell}$$

$$\begin{cases} \alpha = \max\left(0.4\tan^{-1}\left(0.34U_{10} - 1.88\right) + 0.39, 0\right) \\ H_{0,SMB} = \dfrac{0.3U_{10}^2}{g}\left[1 - \left\{1 + 0.004\left(\dfrac{Fg}{U_{10}^2}\right)^{1/2}\right\}^{-2}\right] \\ H_{0,swell} = 1.31 + \dfrac{(2.46 - 1.31)U_{10}}{12} \end{cases} \tag{20}$$

$$T_p = \alpha T_{0,SMB} + (1-\alpha) T_{0,swell}$$

$$\begin{cases} \alpha = \max\left(0.4\tan^{-1}\left(0.34U_{10} - 1.88\right) + 0.39, 0\right) \\ T_{0,SMB} = \dfrac{1.37 \cdot 2\pi U_{10}}{g}\left[1 - \left\{1 + 0.008\left(\dfrac{Fg}{U_{10}^2}\right)^{1/3}\right\}^{-5}\right] \\ T_{0,swell} = 8 \end{cases} \tag{21}$$

where F = 235000 m. Figure 10 shows the variation of significant wave height H_S and wave peak period T_p with the mean wind speed at hub height.

5.2. Combination of wind and wave loads

In order to understand the respective contributions of wind and wave, the full dynamic simulations using the wind and wave conditions discussed above are carried out in three sets considering ‘wind only’, ‘wave only’ and ‘wind+wave’. The wind is set to act in the same direction as wave, as shown in Figure 1, which will cause the most unfavourable load on tower.

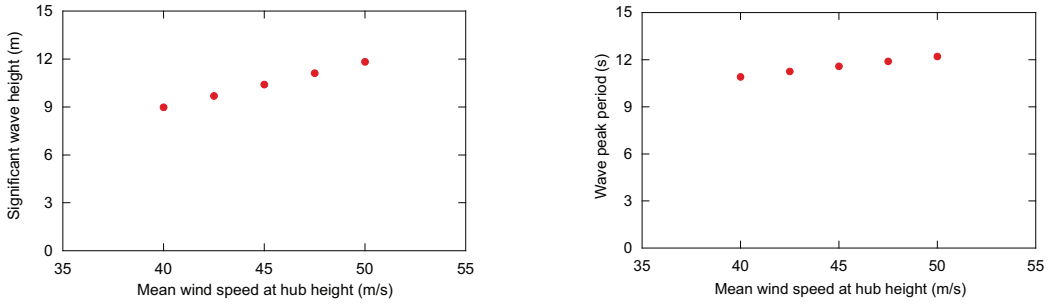

(a) Significant wave height (b) Wave peak period

Figure 10. Significant wave height H_S and wave peak period T_P

The mean svalue and standard deviation of tower base bending moment are compared for the three sets of environmental conditions, as shown in Figure 11. It is indicated that the mean bending moment depends on the wind, and the wave doesn't cause any mean loading. It is found from the comparison of standard deviation that wave contributes more than wind to the dynamic loading. That is why the wave-induced load has to be taken into account for floating wind turbine system. Therefore, the combined tower loading can also be calculated by quasi-steady analysis using wind-induced mean loading, combined standard deviation and combined peak factor.

In the 'wind+wave' case, the general equation of motion can be expressed as:

$$M\ddot{x} + C\dot{x} + Kx = F_{wave} + \frac{1}{2}C_d\rho A\left(U^2 + u^2 + \dot{x}'^2 + 2Uu - 2U\dot{x}' - 2u\dot{x}'\right) + \frac{1}{2}C_d\rho A\left(\dot{s}^2 - 2U\dot{s} - 2u\dot{s} + 2\dot{s}\dot{x}'\right) \quad (22)$$

where F_{wave} is the wave force, C_d is the drag aerodynamic coefficient, ρ is the air density, A is the wind acting area, $x = s + x'$ is the total displacement, s is the displacement due to wave and x' is the displacement due to wind, U is the mean wind speed, u is the fluctuating wind speed. In the right hand side of eqn (22), the second term is the wind force which is totally the same as that of 'wind only' case, defined as F_{wind}; the third term is the coupling aerodynamic force which causes the correlation between wind-induced load and wave-induced load. Since the wave-induced vibration velocity $\dot{s}$ is negligibly small as well as $\dot{x}'$ compared to the mean wind speed in the extreme condition, the second order terms of $\dot{s}^2$, $u\dot{s}$ and $\dot{s}\dot{x}'$ can be neglected in the third term. Therefore, eqn (22) can be decomposed into two equations of motion under wind and wave, respectively:

$$M\ddot{x}' + C\dot{x}' + Kx' = F_{wind}, \quad M\ddot{s} + C\dot{s} + Ks = F_{wave} - C_d\ \rho AU\dot{s} \quad (23a, 23b)$$

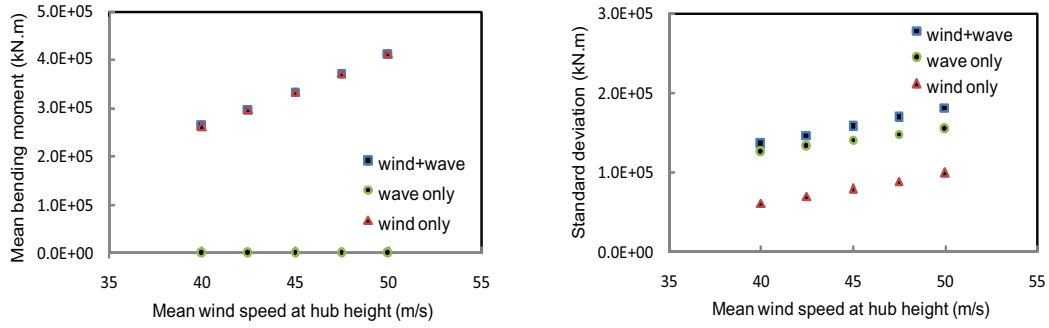

(a) Mean value (b) Standard deviation

Figure 11. Bending moment on tower base

The aerodynamic force $-C_d\rho AU_s$ in eqn (23b) will reduce the wave-induced response. This reduction can be considered by aerodynamic damping. However, the aerodynamic damping ratio is just 1/10~1/20 of the system damping ratio in the SR model for the floating wind turbine, hence can be neglected. Thus, all the coupling aerodynamic forces in the third term of eqn (22) are ignored, which means the correlation between wind-induced load and wave-induced load is neglected as a matter of course. Therefore, the combined standard deviation σ_{cb} is calculated as:

$$\sigma_{cb} = \sqrt{\sigma_{wind}^2 + \sigma_{wave}^2} \tag{24}$$

where σ_{wind} and σ_{wave} are the standard deviations due to wind and wave that are calculated independently in Section 4. It is shown in Figure 12 that the combination without considering any correlation between wind-induced load and wave-induced load can predict the standard deviation of 'wind+wave' case accurately.

The combined peak factor is able to be calculated using eqn (18) of Gaussian peak factor model since the skewness of tower base bending moment of 'wind+wave' case is found to be close to 0 from the full dynamic simulation. In the calculation of zero up-crossing frequency, the wind part is added to the power spectrum:

$$\nu_{0,cb} = \sqrt{\frac{n_{wind}^2\sigma_{wind}^2 + n_p^2\sigma_b^2 + n_s^2\sigma_s^2 + n_t^2\sigma_t^2}{\sigma_{wind}^2 + \sigma_b^2 + \sigma_s^2 + \sigma_t^2}} \tag{25}$$

where $n_{wind}^2\sigma_{wind}^2 = n_{wind,b}^2\sigma_{wind,b}^2 + n_1^2\sigma_{wind,r}^2$, $\sigma_{wind}^2 = \sigma_{wind,b}^2 + \sigma_{wind,r}^2$, $n_{wind,b} = 0.3U_h / \sqrt{L_u\sqrt{A_{wt}}}$. σ_{wind}^2 is the variance of fluctuating wind load; $\sigma_{wind\,b}$ and $\sigma_{wind\,r}$ are the background part and resonant part of wind load standard deviation, respectively; n_1 is the first natural frequency of the floating system; U_h is the mean wind velocity at hub height; L_u is the turbulence integral length scale; A_{wt} is the wind acting area of the whole wind turbine. Figure 13 shows the comparison of proposed formula with full dynamic simulation. It can be seen that the Gaussian model can predict the peak factor of 'wind+wave' case well.

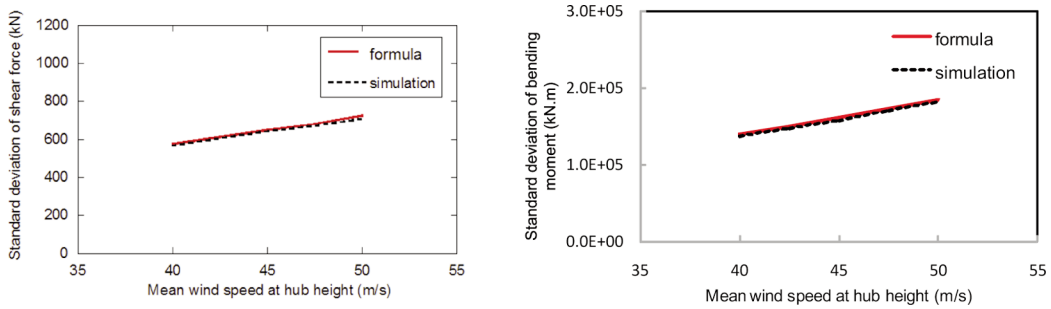

(a) Standard deviation of shear force on tower base (b) Standard deviation of bending moment on tower base

Figure 12. Comparison of combined standard deviation with full dynamic simulation

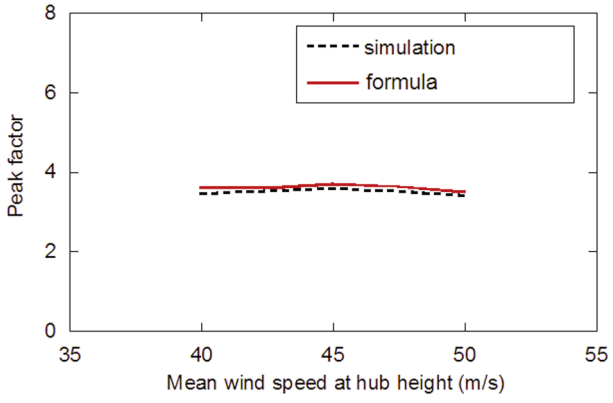

Figure 13. Comparison of combined peak factor with full dynamic simulation

6. CONCLUSIONS

An equivalent SR model is proposed to calculate the tower loading of a floating wind turbine system in the presence of wind and waves. The analytical formulae for the estimation of wind-induced load and wave-induced load are proposed by quasi-steady analysis as well as the formulae for the loads combination. The following conclusions are obtained:

1. The stiffness and damping of surge and pitch modes in the SR model are identified by free vibration simulation.
2. The analytical formulae of wind-induced load are in the same format as those of fixed-foundation wind turbine. The mean value and background standard deviation are the same since they only depend on wind itself; the resonant standard deviation is different because it is the function of the first natural frequency and damping ratio of the system which are much different from the fixed-foundation wind turbine; the non-Gaussian peak factor is found to be not sensitive to the type of foundation.
3. The evaluation formulae of standard deviation of tower loading due to wave-induced floater surge and pitch motions are proposed separately by locking the other motion with modal analysis. Their combination is calculated with CQC rule, and the correlation only depends on the damping and natural frequency of the system. A Gaussian peak factor can be used, since the resonance of floater and tower is only slightly excited by wave.
4. For the total tower loading under wind and wave, the mean value depends on the wind only; the standard deviation can be combined without considering any correlation between wind-induced load and wave-induced load; the Gaussian peak factor is also applicable to the total tower loading.

REFERENCES

[1] Wang, C.M., Utsunomiya, T., Wee, S.C., Choo, Y.S., Research on floating wind turbines: a literature survey. The IES Journal Part A: Civil & Structural Engineering, Vol. 3, No. 4, pp. 267–277, 2010.

[2] Twidell, J., Gaudiosi, G., Offshore Wind Power, Multi-Science Publishing Co. Ltd., UK, 2009.

[3] ISO 3010 Bases for design of structures-Seismic actions on strucures, International Organization for Standardization, Geneva, 2001.

[4] Xu, N., Ishihara, T., Prediction of tower loading of wind turbine in the extreme wind condition considering the type of foundation. The Annual Conference of European Wind Energy Association, Vienna, Austria, 2013.

[5] Waris, M. B., Ishihara, T., Dynamic response analysis of floating offshore wind turbine with different types of heave plates and mooring systems by using a fully nonlinear model. Coupled Systems Mechanics, Vol. 1, No. 3, 2012.

[6] Davenport, A.G., Note on the distribution of the largest value of a random function with application to gust loading. In: Proceedings of the Institute of Civil Engineering, pp. 187–196, 1964.

[7] Jonkman, J.M., Dynamic modeling and load analysis of an offshore floating wind turbine, Department of Aerospace Engineering Sciences, University of Colorado, Ph.D. dissertation, 2007.

[8] Inman, D. J., Vibration with Control, John Wiley & Sons Ltd, USA, 2006.

[9] Xu, N., Ishihara, T., Prediction of dynamic response of wind turbine towers in the parked condition. 13th International Conference on Wind Engineering, Amsterdam, Netherland, 2011.

[10] IEC 61400-3, Edition-1: Wind turbines – Part 3: Design requirements for offshore wind turbines, International Electrotechnical Commission, Geneva, 2008.

[11] Chaplin, J. R., http://www.civil.soton.ac.uk/hydraulics/download/downloadtable.htm, 2010.4.

[12] Chakrabarti, S. K., Hydrodynamics of offshore structures, Computational Mechanics Publications, Southampton, 1987.

[13] Recommendations for loads on buildings, Architectural Institute of Japan (AIJ), Tokyo, 2004.

[14] IEC 61400-1, Edition-3: Wind turbines – Part 1: Design requirements, International Electrotechnical Commission, Geneva, 2005.

[15] Offshore Standard DNV-OS-J101, Design of offshore wind turbine structures, Det Norske Veritas AS, Oslo, 2011.

[16] Sverdrup, H.U., Munk, W.H., Wind, sea, and swell; theory of relations for forecasting, U.S. Navy Hydro-graphic Office, H.O. Pub. 601, pp. 1–44, 1947.

[17] Bretschneider, C.L., Revised wave forecasting relationships, Proceedings of 2nd Conference on Coastal Engineering, ASCE, pp. 1–5, 1952.

[18] Bretschneider, C.L., Revisions in wave forecasting: Deep and shallow water, Proceedings of 6th Conference on Coastal Engineering, ASCE, pp. 30–67, 1958.

APPENDIX

This appendix describes the details of the derivation of tower response due to pitch motion in the SR model. Modal analysis is employed here to get the analytical solution.

By locking the surge motion as shown in Figure 4 (b), the modal equation of motion in pitch direction is:

$$M_j^P \ddot{f}_j^P(t) + C_j^P \dot{f}_j^P(t) + M_j^P \omega_j^{P2} f_j^P(t) = \begin{bmatrix} \phi_{nj}^P \\ \vdots \\ \phi_{1j}^P \end{bmatrix}^T \begin{bmatrix} 0 \\ \vdots \\ M_{wave}(t) \end{bmatrix} = \phi_{1j}^P M_{wave}(t) \tag{A.1}$$

where $M_j^P = \sum_{k=1}^{n} m_k h_k^2 \phi_{kj}^{P2}$,

$$C_j^P = \sum_{k=1}^{n} c_k \phi_{kj}^{P2} \quad (c_1 = c_P)$$

M_j^P is the generalized mass, C_j^P is the generalized damping and ω_j^P is the modal natural frequency in radians per second, f_j^P is the modal displacement, $\phi_{kj}^P (k = 1, \cdots, n)$ is the normalized mode shape of the j th mode, and $M_{wave}(t)$ is the equivalent wave moment in pitch direction.

If the wave varies harmonically, the modal displacement $f_j^P(t)$ can be shown as [8]:

$$f_j^P(t) = \phi_{rj}^P M_{wave}(t) \left| H_j^P(\omega) \right| \tag{A.2}$$

where $$\left| H_j^P(\omega) \right| = \frac{1}{M_j^P \omega_j^{P2} \sqrt{\left(1 - \beta_j^{P2}\right)^2 + 4\xi_j^{P2} \beta_j^{P2}}}$$

$$\beta_j^P = \frac{\omega}{\omega_j^P}$$

$$\xi_j^P = \frac{C_j^P}{2M_j^P \omega_j^P}$$

In modal analysis the results of different natural modes are superposed to calculate the real response. Substituting (A.2), the angular acceleration at node r can be calculated as:

$$\ddot{\theta}_r^P = \sum_{j=1}^{n} \ddot{f}_j^P(t) \phi_{rj}^P = -\omega^2 M_{wave}(t) \sum_{j=1}^{n} \left| H_j^P(\omega) \right| \phi_{1j}^P \phi_{rj}^P \tag{A.3}$$